NJC

New Journal of Chemistry

A journal for new directions in chemistry

Accepted Manuscript

This article can be cited before page numbers have been issued, to do this please use: J. ernák, K. Hararová, L. R. Falvello, L. Dlhá, J. Titis and R. Boca, *New J. Chem.*, 2020, DOI: 10.1039/D0NJ02276D.

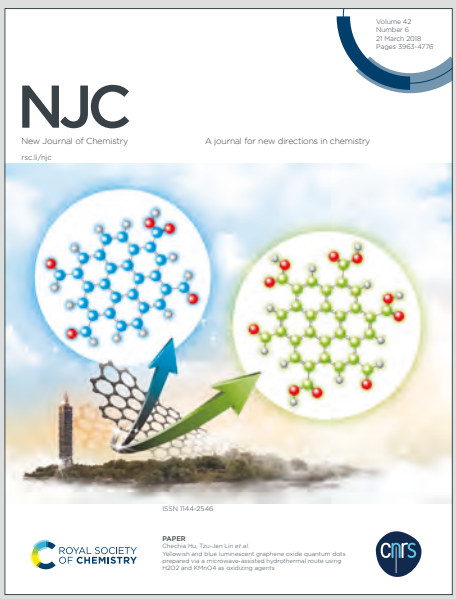

This is an Accepted Manuscript, which has been through the Royal Society of Chemistry peer review process and has been accepted for publication.

Accepted Manuscripts are published online shortly after acceptance, before technical editing, formatting and proof reading. Using this free service, authors can make their results available to the community, in citable form, before we publish the edited article. We will replace this Accepted Manuscript with the edited and formatted Advance Article as soon as it is available.

You can find more information about Accepted Manuscripts in the Information for Authors.

Please note that technical editing may introduce minor changes to the text and/or graphics, which may alter content. The journal's standard Terms & Conditions and the Ethical guidelines still apply. In no event shall the Royal Society of Chemistry be held responsible for any errors or omissions in this Accepted Manuscript or any consequences arising from the use of any information it contains.

View Article Online
DOI: 10.1039/D0NJ02276D

ARTICLE

Field induced slow magnetic relaxation in a zig-zag chain-like Dy(III) complex with the ligand *o*-phenylenedioxydiacetato

Received 00th January 20xx,
Accepted 00th January 20xx

DOI: 10.1039/x0xx00000x

Juraj Černák,*[a] Katarína Harčarová, [a] Larry R. Falvello, [b] Ľubor Dlháň, [c] Ján Titiš [d] and Roman Boča [d]

The new complex $[Dy(PDOA)(NO_3)(H_2O)_2]_n \cdot nH_2O$ (**1**) (H_2PDOA is *o*-phenylenedioxydiacetic acid) was isolated from the reaction of dysprosium(III) nitrate and H_2PDOA in a 1:1 molar ratio. Its crystal structure is formed of neutral *zig-zag* chains in which the nona-coordinated Dy(III) atoms (O_9 donor set) are linked by *PDOA* ligands with a chelating-bridging coordination mode. DC and AC magnetic studies revealed that **1** behaves as a field-induced SMM with three relaxation channels. The derived values, considering the Orbach relaxation process, of the barrier to spin reversal and the extrapolated relaxation time are U/k_B = 59.5 K and $\tau_0 = 6.3 \times 10^{-10}$ s, respectively. *Ab initio* calculations support the experimental results.

Introduction

Since the discovery of Single Molecule Magnets (SMM)[1] the lanthanide complexes have been intensively studied, as the significant magnetic anisotropy and large magnetic moments of the lanthanide centers make them ideal candidates for SMMs.[2] The main driving force for such studies include the potential applications of magnetic materials based on lanthanides (and other entities) in the area of high density data storage, spintronics and quantum computing.[3] The key indicator for suitable SMMs is the effective energy barrier for reversal of magnetization, U_{eff}. Attaining the highest possible value of this indicator is one of the main challenges in inorganic chemistry at present.

Among the lanthanide ions, Dy(III) and its complexes are good candidates for the preparation of SMMs as Dy(III) displays bistable ground state spin and a high magnetic anisotropy arising from the $^6H_{15/2}$ state.[4] Factors that enable the tuning of the magnetic anisotropy of the Dy(III) complexes include the composition of the coordination sphere (usually O-donor ligands) and its symmetry; and an important role can also be played by the intra- and intermolecular interactions.[5] As a consequence, the quest for SMM based on Dy(III) has resulted in a large number of Dy(III) complexes having been synthesized and studied during the last few years.[2a,5b,6] At present, to the best of our knowledge, the highest value of the energy barrier U_{eff} = 2217 K (1541 cm^{-1}), with the blocking temperature T_B = 80 K, was achieved for a Dy(III) metallocene cation $[(Cp^{iPr5})Dy(Cp^*)]^+$ (Cp^{iPr5} = penta-iso-propylcyclopentadienyl, Cp^* = pentamethylcyclopentadienyl).[7]

From a structural point of view Dy(III) complexes can be mononuclear, polynuclear, with the simplest case being dinuclear, or polymeric. Mononuclear complexes are suitable for attaining high values of U_{eff}, so it is not surprising that the highest value was reported for this type of dysprosium(III) complexes.[2e,7,8] The dinuclear {Dy_2} complexes are interesting as they can be used to study the influence of the exchange interaction between the lanthanide ions on the SMM properties.[4a,5b,6c,9] Dy(III) complexes with various higher nuclearities up to {Dy_{76}} have also attracted broad interest.[2e,6a,6b,10] The disadvantage of these Dy(III) complexes with various high nuclearities is usually low SMM activity due to the presence of fast quantum tunnelling.[6a,6d,11] A large number of Dy(III) complexes with polymeric structures have been studied, too.[6g,12] In these complexes the Dy···Dy interatomic distances seems to be an important parameter. In the case of short bridging the contribution from the exchange interactions can be important, while those with longer separations between the Dy(III) atoms, due to negligible exchange interactions, behave effectively as SIMs.[6g,13]

An efficient multi *O*-donor ligand for the synthesis of lanthanide complexes is *PDOA* (H_2PDOA is *o*-phenylenedioxydiacetic acid). A search in the Cambridge Structural Database (CSD)[14] yielded 36 hits for a combination of the *PDOA* ligand and a lanthanide atom. Various coordination modes were found, e.g. tetradentate chelating in $[Yb_2(PDOA)_3(H_2O)_6]\cdot 4H_2O$,[15] pentadentate chelating-bridging in $[Ce(PDOA)(NO_3)(H_2O)_3]\cdot H_2O$,[16] hexadentate chelating-bridging in $[Pr(PDOA)(NO_3)(H_2O)_2]$,[17] or purely bridging *PDOA*

[a] Department of Inorganic Chemistry, Faculty of Sciences, P. J. Šafárik University in Košice, Moyzesova 11, 041 54 Košice, Slovakia.
[b] Departamento de Química Inorgánica, Instituto de Ciencia de Materiales de Aragón (ICMA), University of Zaragoza-CSIC, Pedro Cerbuna 12, E-50009 Zaragoza, Spain.
[c] Institute of Inorganic Chemistry, Slovak University of Technology, Radlinského 9, 812 37 Bratislava, Slovakia.
[d] Department of Chemistry, Faculty of Natural Sciences, University of SS Cyril and Methodius, nám. J. Herdu 2, 917 01 Trnava, Slovakia.
Present address of KH: Environmental Department, Faculty of Civil Engineering, Technical University in Košice, Slovakia.
† Electronic Supplementary Information (ESI) available: For additional spectroscopic, crystallographic and magnetic data and figures see DOI: 10.1039/x0xx00000x

DOI: 10.1039/D0NJ02276D

coordinated in a bis(chelating)-fashion in $[Dy_2(PDOA)_3(H_2O)_6]\cdot 3.5H_2O$[6g] or in a bis(monodentate) fashion in $[Sm_2(PDOA)_3(H_2O)_6]\cdot 2H_2O$.[18] It should be noted that often two different bonding modes are present in the same crystal structure.

We have previously synthesized and structurally characterized two Dy(III) complexes with *PDOA*, namely the polymeric complex $\{[Dy_2(PDOA)_3(H_2O)_6]\cdot 2H_2O\}_n$ with a ladder-like arrangement of Dy(III) atoms and its dinuclear analogue $[Dy_2(PDOA)_3(H_2O)_6]\cdot 3.5H_2O$. Both complexes exhibited field-induced slow magnetic relaxation with similar quantitative characteristics.[6g] In the present study we report our results on the synthesis and characterization of the new complex $[Dy(PDOA)(NO_3)(H_2O)_2]_n\cdot nH_2O$ (**1**) along with its crystal structure, and static/dynamic magnetic properties.

Results and discussion

Synthesis and identification

From the mostly ethanolic reaction system (ethanol:water vv ratio was 15:1) containing dysprosium nitrate hexahydrate and H_2PDOA in molar ratio 1:1 under mild conditions (reflux) the title complex $[Dy(PDOA)(NO_3)(H_2O)_2]_n\cdot nH_2O$ (**1**) separated (Fig. 1). Previously, from an analogous aqueous reaction mixture with a molar ratio of 2:3 for the starting materials, a dihydrate $\{[Dy_2(PDOA)_3(H_2O)_6]\cdot 2H_2O\}_n$ (CSD refcodes NUDWAL01 for T = 173 K and NUDWAL for T = 296 K) with a ladder-like crystal structure was isolated.[6g,18] The addition of *bpy* to the reaction mixture (*bpy* = 2,2'-bipyridine), intended as an auxiliary ligand, resulted in the isolation of a higher hydrate $[Dy_2(PDOA)_3(H_2O)_6]\cdot 3.5H_2O$ (LATKUP) with a dinuclear structure, in which, however, the *bpy* did not enter into the final product.[6g] These results indicate that in the presence of a sufficient amount of the *PDOA* ligand (here 1.5 mole per mole of Dy(III)), this ligand is preferentially used for saturation of the coordination sphere of the Dy(III) atom as well as for compensation of the +3 charge of the central atom. On the other hand, the use of a lower *PDOA*:Dy molar ratio (1:1) led to incorporation of the nitrate anion as an additional co-ligand fulfilling both purposes, charge compensation as well as saturation of the coordination sphere of the Dy(III) atom. We note here that there was a previous report of a Dy(III) complex with *PDOA* and with *phen* (*phen* = 1,10-phenantroline) as an auxiliary ligand (VODGOL).[19]

The IR spectrum of **1** is rich in information; the positions of the absorption bands are gathered in the experimental section. A characteristic signal is a broad, strong absorption band centred around 3376 cm^{-1} which in accord with the literature[20] was assigned to ν(OH) vibrations of the water molecules. Further characteristic absorption bands are those arising from asymmetric and symmetric vibrations ν(COO) of the carboxylate groups. Their positions at 1597 and 1458 as well as at 1433 cm^{-1} are in line with the corresponding bands found at 1580 cm^{-1} and 1433 cm^{-1} in the analogous $\{[Dy_2(PDOA)_3(H_2O)_6]\cdot 2H_2O\}_n$.[6g] The presence of aromatic rings manifests itself by sharp absorption bands observed at 1500 cm^{-1}; the corresponding band was observed at 1499 cm^{-1} in the IR spectrum of $\{[Dy_2(PDOA)_3(H_2O)_6]\cdot 2H_2O\}_n$].[6g]

The phase identity and purity of the bulk sample was corroborated by powder diffraction methods. Figure S1 shows a comparison of the experimental diffraction pattern and that modelled by LeBail profile fitting.[21] It is worth noting that the unit cell volume using the LeBail method (1480.3 $Å^3$, T = 295 K) is larger than the cell volume from single crystal data (1472.6 $Å^3$, T = 123 K; Table S1) in line with the temperature change.

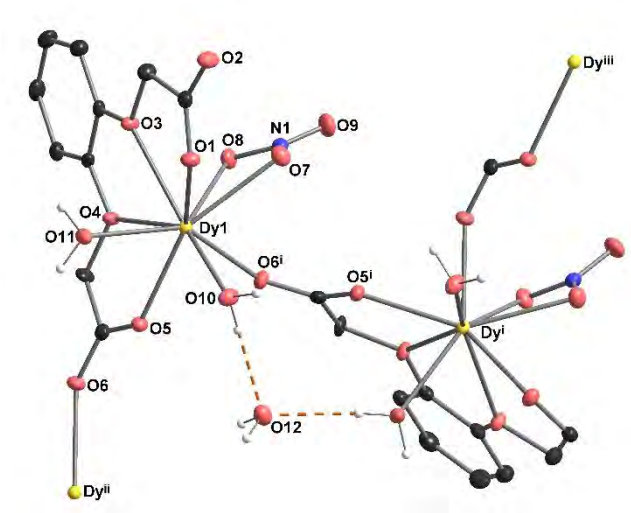

Fig. 1. *Zig-zag* chain formed by Dy(III) atoms in **1**. The thermal ellipsoids are drawn at 50 % probability level. Hydrogen atoms bonded to carbon atoms are omitted for clarity. Dashed lines represent hydrogen bonds. Symmetry codes: i: x, 0.5 – y, –0.5 + z; ii: x, 0.5 – y, 0.5 + z; iii: x, y, z - 1.

Crystal structure

The crystal structure of **1** is comprised of Dy(III) atoms which are linked by the bridging-chelating ligand *PDOA* into zig-zag chains running along the *c*-axis (Fig. 1, Fig. S2); the crystal structure is completed by one water solvate molecule per formula unit. Similar zig-zag chains were reported in the analogous Ce(III) complex $[Ce(PDOA)(NO_3)(H_2O)_3]\cdot H_2O\}_n$ (VOWDOC) in which a chelating nitrato ligand also entered into the Ce(III) coordination sphere;[16] the main difference with respect to **1** is that the Ce(III) atom upon coordination of three aqua ligands exhibits deca-coordination, presumably due to its larger ionic radius (1.25 Å) with respect to the smaller Dy(III) atom (1.083 Å).[22] Incorporation of a nitrato co-ligand in the coordination sphere of lanthanide complexes with *PDOA* was reported in five additional complexes with general formula $[Ln(PDOA)(NO_3)(H_2O)_2]$, namely in complexes with Ln = Ce, (VOWDIW, VOWDIW01),[16,17] Ln = La $[La(PDOA)(NO_3)(H_2O)_2]$ (UWAJUZ),[17] Ln = Pr $[Pr(PDOA)(NO_3)(H_2O)_2]$ (UWAJOT),[17] and Ln = Gd $[Gd(PDOA)(NO_3)(H_2O)_2]$ (FAKKAG).[23]

The Dy1 central atom is nona-coordinated by four oxygen atoms from the triply chelating *PDOA* ligand, two aqua ligands, one chelating nitrato ligand and an additional oxygen atom from the bridging function of the neighbouring *PDOA* ligand, yielding an $O_4O'_2O''_2O'''$ donor set. As analysed by the program *SHAPE*[24] the shape of the DyO_9 coordination polyhedron approximates to a muffin shape (symmetry C_s) (Fig. 2).

View Article Online
DOI: 10.1039/D0NJ02376D

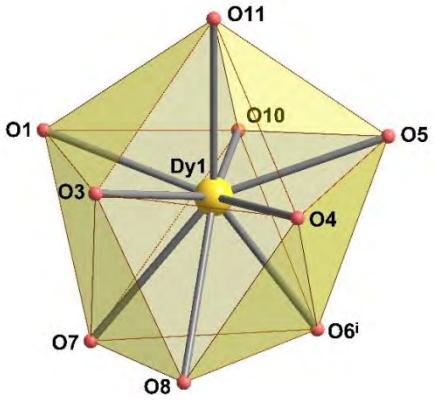

Fig. 2. View of the coordination polyhedron of the Dy(III) atom in **1**. Symmetry code: i: *x*, 0.5 – *y*, –0.5 + *z*.

The Dy–O bond lengths (Table 1, Table S2) lie in the range 2.3150(18) (O10 aqua ligand)-2.606(2) Å (O8 atom from the nitrato ligand). In the similar complex $\{[Dy_2(PDOA)_3(H_2O)_6]\cdot 2H_2O\}_n$ the Dy-O bonds fall into a somewhat broader range, 2.2652(17) – 2.6477(16) Å.[6g] Noteworthy is the marked asymmetry (2.4898(19) Å and 2.606(2) Å) of the two Dy-O bonds in **1** from the chelating nitrato ligand. Similar values of 2.482(5) and 2.608(5) Å for Dy-O bonds from a chelating nitrato ligand were reported for $[NHEt_3]_2[Dy_2(\mu\text{-}NO_3)_2(NO_3)_2(HL)_2]$ (*Et* = ethyl, H_3L=N′-(2-hydroxy-3-methoxy-5-nitrobenzylidene)-2-(hydroxyimino) propanehydrazide).[25] The mean O-Dy-O bite angle of the chelate rings in the *PDOA* ligand is 64.85° while the corresponding angle within the nitrato ligand (49.98(6)°) is considerably more acute. These values are close to those of 63.11° and 49.71(16)° found in the analogous complexes $\{[Dy_2(PDOA)_3(H_2O)_6]\cdot 2H_2O\}_n$ and $[NHEt_3]_2[Dy_2(\mu\text{-}NO_3)_2(NO_3)_2(HL)_2]$, respectively.[6g,25]

Table 1 Dy-O bond distances (Å) in **1**.

Dy1-O1	2.3398(18)	Dy1-O3	2.4699(17)
Dy1-O4	2.4321(17)	Dy1-O5	2.3350(17)
Dy1-O6i	2.3308(18)	Dy1-O7	2.4898(19)
Dy1-O8	2.606(2)	Dy1-O10	2.3150(18)
Dy1-O11	2.4024(18)		

Symmetry code: i: *x*, 0.5 – *y*, –0.5 + *z*.

The space between the zig-zag chains is occupied by O-H···O hydrogen bonds with participation of aqua ligands, the water solvate molecule and some oxygen atoms from carboxylate and nitrate groups (Table S3, Figure S2). The geometric parameters associated with these HBs (O···O distances are in the range 2.701(3) - 2.891(3) Å and the O-H···O angles exhibit values in the range 158(3)-175(3)°) indicates their medium strength. These hydrogen bonds mediate an approach of the Dy(III) atoms in the neighbouring chains, with a shortest inter-chain Dy···Dy^{iv} (iv: -*x*, -*y*, -*z*) distance of 7.0295(3) Å; this value is rather close to the distance between the Dy(III) atoms within the chains, 6.1978(3) Å.

Magnetic properties

The molar magnetic susceptibility for **1** has been transformed to the effective magnetic moment and its temperature dependence is shown in Fig. 3. The room temperature value μ_{eff} = 10.5 μ_B stays almost constant down to T ~ 100 K when it gradually decreases to μ_{eff} = 9.6 μ_B. The molar magnetic susceptibility on cooling increases monotonically over the whole temperature range.

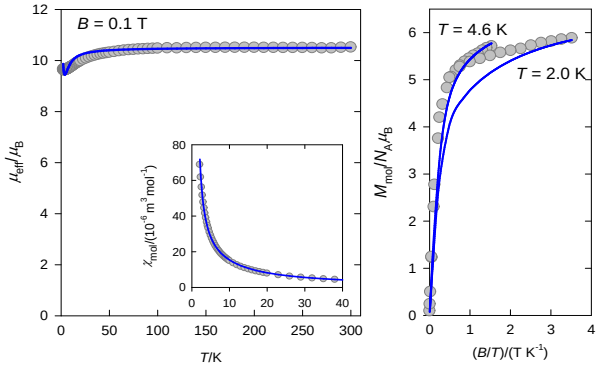

Fig. 3. Temperature dependence of the effective magnetic moment (left) and the field dependence of the magnetization per formula unit (right). Full lines – fitted.

The single Dy(III) centre possessing the electronic ground multiplet $^6H_{15/2}$ implies j_{Dy} = 15/2, and g_{Dy} = 4/3 and thus the high-temperature value of $\mu_{eff}(HT) = g[j(j+1)]^{1/2}$ = 10.6 μ_B. The magnetization per formula unit adopts a value of $M_1 = M_{mol}/N_A\mu_B$ = 5.9 at B = 7.0 T and T = 2.0 K. The expected saturation value at high field is M_1(HF)= $j\cdot g$ = 10. However, the multiplet splitting causes a marked reduction at low temperatures.

The DC susceptibility and magnetization data were fitted simultaneously by employing a simple spin Hamiltonian [#]

$$\hat{H} = \mu_B g_J B_z \hat{J}_z \hbar^{-1} + \Delta(\hat{J}_z^2 - \hat{J}^2/3)\hbar^{-2} \quad (1)$$

with J = 15/2 and Δ representing an axial distortion parameter. The fitting procedure converged to g_J = 1.314 and Δ/hc = 9.7 cm^{-1}. A small molecular field correction zj/hc = 0.024 cm^{-1} reproduces a hook in the low-temperature effective magnetic moment. A similar hook for $\chi_M.T$ values between 4.25 and 1.8 K was observed for the polymeric Dy(III) complex with a similar chromophore $DyO_2O_2O_5$ arising from *MSA*, two aqua and one chelating nitrato ligands, namely $\{[Dy(MSA)(NO_3)(H_2O)_2]\cdot 2H_2O\}$ (H_2MSA = 2-methylenesuccinic acid; [Dy-MSA]$_n$).[26]

The AC susceptibility data was taken first at low temperature T = 2.0 K and a set of four representative frequencies of the oscillating magnetic field; the B_{DC} rises to 1.0 T (Fig. 4). There is no evidence for an out-of-phase susceptibility signal at zero field. The same behaviour was observed for two other Dy(III) complexes with *PDOA* ligands with known crystal structures, namely $\{[Dy_2(PDOA)_3(H_2O)_6]\cdot 2H_2O\}_n$ [Dy$_2$]$_n$ with a ladder-like crystal structure and its dinuclear analog $[Dy_2(PDOA)_3(H_2O)_6]\cdot 3.5H_2O$ ([Dy$_2$]).[6g] On the other hand, in the above mentioned [Dy-MSA]$_n$ complex the presence of one relaxation process at zero-field was reported.[26]

It can be seen from Fig. 4 that the maximum of the out-of-phase susceptibility χ'' for **1** appears at *ca* B_{DC} = 0.15 T and then the response attenuates progressively with the magnetic field. This field has been selected for the detailed mapping as follows.

View Article Online
DOI: 10.1039/D0NJ02276D

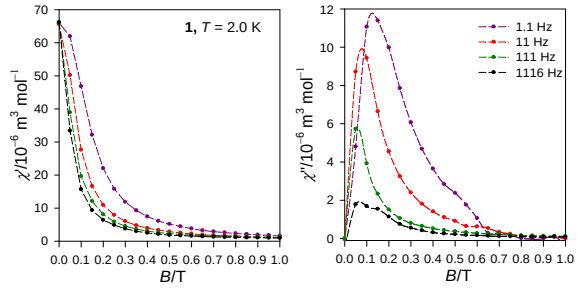

Fig. 4. The AC susceptibility components for **1** as functions of the B_{DC} field at T = 2.0 K.

Temperature evolution of the AC susceptibility components is presented in Fig. 5 for 20 frequencies ranging between f = 0.1 and 1000 Hz. It can be seen that the devitrification point, when the in-phase components merge and the out-of-phase components vanish, is at ca 7 K. Above this temperature the usual paramagnetic behaviour occurs.

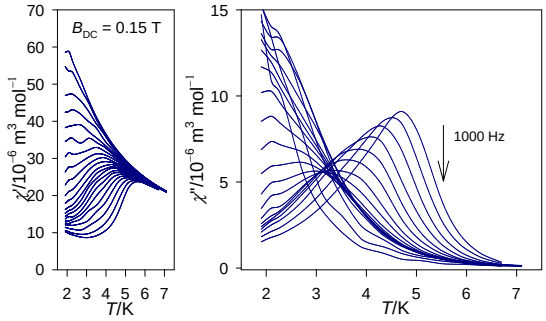

Fig. 5. Temperature dependence of the in-phase and the out-of-phase susceptibility for various frequencies f = 0.1 – 1000 Hz.

The same data set has been rearranged to obtain Fig. 6 where the susceptibility components are plotted as functions of the frequencies f of the oscillating field for a set of temperatures. Just this function can be fitted to an extended Debye model. Since three maxima are visible in the out-of-phase susceptibility, the three-set Debye model containing 10 free parameters has been applied: the adiabatic susceptibility χ_S, three isothermal susceptibilities χ_{Tk}, three distribution parameters α_k, and three relaxation times τ_k. Note that there are 40 experimental points for each temperature so that there is no overparameterization. A standard deviation is associated with each free parameter as listed in the ESI.

It can be seen that at low temperature T = 1.9 K the low-frequency (LF) and the intermediate-frequency (IF) relaxation channels prevail and the data analysis yields the mole fractions x(LF) = 0.39 and x(IF) = 0.54. The corresponding relaxation times are as long as τ(LF) = 1.17(7) s and τ(IF) = 0.088(16) s, respectively. Under the same conditions, the high-frequency relaxation time is as short as τ(HF) = 0.36(9) ms. On heating, dramatic changes are visible: (i) the height of the LF and IF peaks (referring to the isothermal susceptibilities) rapidly decrease which manifest themselves in a rapid decrease of the mole fractions x(LF) and x(IF); at the same time the height of the HF peak increases until a maximum and then it disappears as well.

The existence of multiple relaxation processes in the case of Dy(III) based SMMs is not uncommon, especially in the case of Dy(III) complexes containing several crystallographically independent metal centres. By way of example, we can mention a dinuclear complex $[Dy_2Lz_2(C_6H_5CO_2)_6]\cdot 2CH_3CN$ (*Lz* = 6-pyridin-2-yl-[1,3,5]triazine-2,4-diamine),[27] the tetranuclear complex $[Dy_4(L)_4(HL)_2(C_6H_4NH_2COO)_2(CH_3OH)_4]\cdot 5CH_3OH$ (H_2L = N-(2-carboxyphenyl)salicylidenimine),[28] or the heptanuclear complex $[(Co_4Dy_3L_4)DyL(O)_2(OMe)_2(ac)_4(H_2O)_2(NO_3)_2](NO_3)\cdot 3CH_3OH \cdot 1.5H_2O$ (where H_2L is the [1+1] condensation product of 3-methoxysalicylaldehyde and 2-amino-2-methyl-1-propanol).[29] We note that in both analogous Dy(III) complexes containing *PDOA* ligands, $[Dy_2]_n$ and ([Dy$_2$], only two relaxation processes were observed.[6g]

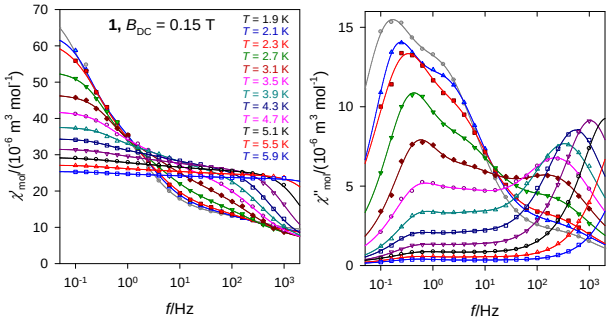

Fig 6. Frequency dependence of the susceptibility components for fixed temperature. Lines – fitted.

The fitted data was used in constructing the Argand diagram (Fig. 7 – left) and the Arrhenius-like plot (Fig. 7 – right). Three high-temperature data of the HF channel have been used for a linear fit, $\ln\tau$ = b[0] + b[1]T^{-1}, which allows an estimate of the barrier to spin reversal and the extrapolated relaxation time when the Orbach relaxation process $\tau = \tau_0\exp(U/k_BT)$ is considered: U/k_B = 59.5 K and τ_0 = 6.3 × 10^{-10} s. A somewhat higher barrier to spin reversal associated with analogous relaxation times (71.6 K and 6.3 × 10^{-10} s; 97.8 K and 2.4 × 10^{-11} s) were observed in similar Dy(III) complexes with the *PDOA* ligand, $[Dy_2(PDOA)_3(H_2O)_6]\cdot 2H_2O$ and $[Dy_2(PDOA)_3(H_2O)_6]\cdot 3.5H_2O$, respectively.[6g]

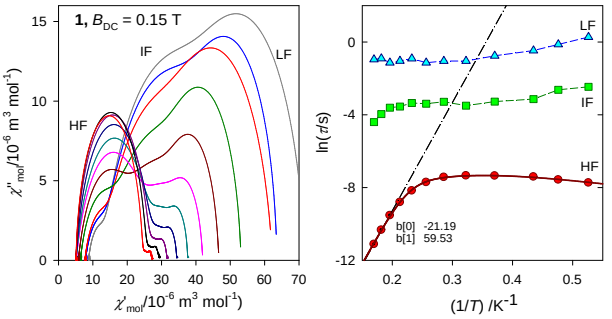

Fig. 7. The Argand diagram (left); Arrhenius-like plot (right), full curved line – fitted, dot-dashed – high-temperature (Orbach-only) process.

Careful inspection of Fig. 7 shows an unexpected effect: on cooling the relaxation time referring to the HF channel is shortened. This *reciprocating thermal behaviour* is better seen in Fig. 8. The experimental data was fitted to an extended relaxation formula

$$\tau^{-1} = \tau_0^{-1}\exp(-U/k_BT) + CT^l + E_sT^{-k} \quad (2)$$

which includes the Orbach process, the phonon bottleneck process, and the "strange" relaxation process.[6f,30-34] The fitting procedure gave U/k_B = 60(3) K, τ_0 = 6(3) × 10^{-10} s, C = 193 K^{-l} s^{-1}, l = 1.56, E_s = 1.0 × 10^4 K s^{-1}, and k = 2.8. The Orbach-process parameters match the high-temperature approximation and the small value of the exponent l confirms that the phonon bottleneck process applies instead of the formally analogous Raman term. The "strange" process needs to be added in order to reproduce the low-temperature data. Most probably this refers to the second solution for the phonon bottleneck process.[35]

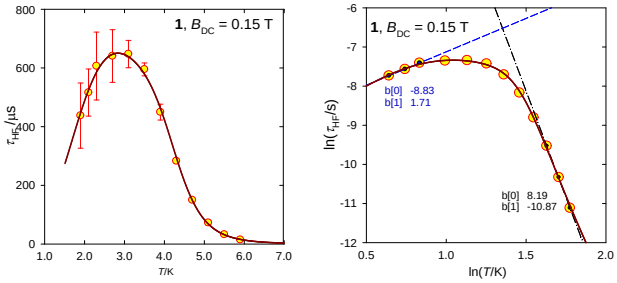

Fig. 8. The temperature evolution of the relaxation time for the high-frequency relaxation channel. Full curve – fitted by eqn (2).

A literature survey has shown that among the nona-coordinated Dy(III) complexes with a similar coordination environment (one chelating nitrato ligand, at least two aqua ligands and additional O-donor ligands with a $DyO_2O_2O_5$ chromophore, slow magnetic relaxation was reported only for two complexes. AC magnetic measurements of the previously mentioned {[Dy(*MSA*)$(NO_3)(H_2O)_2$]·$2H_2O$} indicated the presence of only one relaxation process at zero-field and the calculated values of the energy barrier and relaxation time were 1.88 K and 0.24 × 10^{-6} s, respectively.[26] In the case of the second complex, namely {$Dy_2(NO_3)_2(H_2O)_{10}$(*CB[6]*)}·$4NO_3$·$14H_2O$ (*CB[6]* = cucurbit[6]uril) with a dinuclear structure, under an applied field of 1000 Oe only a weak out-of-phase signal was observed, so its field-induced SMM nature is questionable.[36]

Ab initio calculations on complex **1** yielded the value of 10.6 μ_B for the calculated effective magnetic moment at room temperature (Fig. S3). On cooling, the value of μ_{eff} gradually decreases, roughly following the experimental behaviour. The magnetization adopts a value of $M_{mol}/N_A\mu_B$ = 5.1 at B = 7.0 T and T = 2.0 K, which again corresponds to the experiment. The calculated values of the g-factor components reflect considerable magnetic anisotropy (g_1 1.51, g_2 1.99, g_3 4.68) (Table S5). The ground electronic multiplet for the Dy(III) ion is $^6H_{15/2}$ which is further split by the effect of the ligand field (DyO_9) to m_j states. The calculated SOC corrected energies of multiplets within all considered states are shown in Table S6. Kramers doublets of the j_{Dy} = 15/2 ground multiplet form an energy barrier for spin reorientation whose height is Δ = 586 cm^{-1} (Fig. S5). To clarify the magnetic relaxation, the transition magnetic moments were also calculated which suggest fast tunnelling processes especially for Kramers doublets with higher energies.

Experimental

Materials and methods

Dysprosium(III) nitrate hexahydrate, $Dy(NO_3)_3·6H_2O$ (99.99 %), *o*-phenylenedioxydiacetic acid, H_2*PDOA* (98 %), ethanol (99.8 %) and sodium hydroxide, NaOH (p.a.) were purchased from commercial sources and used as received.

CHN analysis was carried out on an Elementar vario MICRO analyser. Infrared spectra were recorded on a Bruker Tensor 27 FT-IR (Bruker Optik GmbH., Germany) spectrometer using the KBr technique in the range of 4000 – 400 cm^{-1}. X-ray powder patterns were measured on a RIGAKU D-Max/2500 diffractometer with rotating anode and RINT2000 vertical goniometer, in the 2θ range 5–50 ° using a step of 0.02° and Cu $K_{\alpha 1}$ radiation (λ = 1.54059 Å). The measured powder diffraction pattern was fitted by the LeBail method[21a] incorporated in the program JANA2006.[21b]

Single-crystal X-ray data were collected at 123(2) K on an Oxford Diffraction Xcalibur diffractometer equipped with a Sapphire3 CCD detector and a graphite monochromator utilizing Mo-K_α radiation (λ = 0.71073 Å). Absorption corrections were based on the multi-scan technique using CrysAlisPro.[37] It was possible to index a minor second component, estimated at approximately 6% of the volume of the sample. This was included in the integration step, in order to ameliorate any effects of reflection overlap. Nevertheless, the separation of the major and minor domains was sufficient to permit the obtention of a single-domain data set, complete to beyond 0.84 Å resolution and with average redundancy greater than 10, for the major component alone. That data set was used for structure solution and refinement. The structure was solved by SIR92[38] and refined against the F^2 data using full-matrix least squares methods with the program SHELXL-2018/3.[39] Anisotropic displacement parameters were refined for all non-hydrogen atoms. The hydrogen atoms bonded to carbon atoms were included at idealized positions and refined as riders with isotropic displacement parameters assigned as 1.2 times the U_{eq} values of the corresponding parent atoms. Hydrogen atoms of the aqua ligands and water molecules were located in a difference map and refined with restrained geometry and constrained isotropic thermal parameters with U_{iso}(H) set to 1.5U_{eq} of the parent oxygen atoms. The crystal and experimental data are given in Table S1 and selected geometric parameters are given in Tables 1 and S2. Possible hydrogen bonds are gathered in Table S3. Some geometric parameters were calculated using the program *PARST*.[40] The structural figures were drawn using *Diamond*.[41]

CCDC 1992422 (complex **1**) contains the supplementary crystallographic data for this paper. These data can be obtained free of charge *via* http://www.ccdc.cam.ac.uk/conts/retrieving.html, or from the Cambridge Crystallographic Data Centre, 12 Union Road, Cambridge CB2 1EZ, UK; fax: (þ44) 1223-336-033; or e-mail: deposit@ccdc.cam.ac.uk.

Magnetic data were measured on a SQUID magnetometer (MPMS-XL7, Quantum Design) using the RSO mode of detection with ca 40 mg of the sample encapsulated in a gelatin sample holder. The magnetic susceptibility taken at B = 0.1 T was corrected for the underlying diamagnetism. AC susceptibility

measurements were done with an oscillating field B_{AC} = 0.38 mT for twenty frequencies ranging between f = 0.1 –1000 Hz and a temperature interval T = 1.9 – 7.0 K; 10 scans were averaged for each temperature-frequency point. The use of a small DC magnetic field B_{DC} = 0.15 T was essential to yield the out-of-phase susceptibility response.

Ab initio calculations

Ab initio calculations were performed with the ORCA 4.2.1 computational package using the truncated experimental geometry of complex **1** (monomeric Dy unit).[42] The relativistic effects were included in the calculations with the second-order Douglas-Kroll-Hess (DKH)[43] procedure together with the scalar relativistic contracted version of the def2-SV(P) basis function for all elements, except the Dy atom. For Dy, the SARC2-DKH-QZVP basis function was used.[44] The calculations were based on state average complete active space self-consistent field (SA-CASSCF) wave functions. The active space of the CASSCF calculations for **1** was comprised of nine electrons in seven metal-based *f*-orbitals. The state averaged approach was used, in which 21 sextet states were equally weighted. The spin-orbit effects were included through quasi-degenerate perturbation theory in which an approximation to the Breit-Pauli form of the spin-orbit coupling operator (SOMF) was utilized.[45]

Synthesis of [Dy(*PDOA*)(NO$_3$)(H$_2$O)$_2$]$_n$·*n*H$_2$O (1)

0.228 g Dy(NO$_3$)$_3$·6H$_2$O (0.5 mmol), 0.113 g H$_2$*PDOA* (0.5 mmol), 15 ml of ethanol and 1 ml of a 1 M aqueous solution of NaOH were placed in a 50 ml boiling flask. The mixture was heated under reflux with stirring for 1 hour. The precipitated white powder was separated from the colourless solution by filtration (yield 20 %) and after several days colourless crystals suitable for a single crystal study separated from the filtrate. Yield: 13 % (crystals).

Conclusions

Under mild conditions the title complex [Dy(*PDOA*)(NO$_3$)(H$_2$O)$_2$]$_n$·*n*H$_2$O (**1**) was isolated from the system based on dysprosium(III) nitrate and *PDOA* in molar ratio 1:1. A single crystal X-ray study revealed that its crystal structure is built up of electroneutral *zig-zag* chains with Dy(III) atoms nona-coordinated (O$_9$ donor set) by one chelating nitrato ligand, two aqua ligands and a *PDOA* ligand with a chelating-bridging coordination mode. A magnetic study revealed that **1** exhibits a field-induced slow magnetic relaxation characterized by three relaxation channels. The relaxation time associated with the low-frequency channel is as long as τ(LF) = 1.17(7) s, and the corresponding mole fraction is x(LF) = 0.39 at T = 1.9 K with an external field B_{DC} = 0.15 T. On heating this channel is suppressed in favour of the high-frequency channel. The relaxation time referring to the HF channel is shortened on cooling. High-temperature & high-frequency data yield the parameters of the Orbach relaxation process: U/k_B = 44.6 K and $\tau_0 = 1.1 \times 10^{-8}$ s. The experimental magnetic data were corroborated by theoretical calculations.

Conflicts of interest

There are no conflicts to declare.

Acknowledgements

Financial support from Slovak grant agencies (APPV-18-0016 and VEGA 1/0063/17) is gratefully acknowledged. We also thank the Ministerio de Ciencia e Innovación (Spain, Grant PGC2018-093451-B-I00), the European Union Regional Development Fund, FEDER), and the Diputación General de Aragón, Project M4, E11_20R. We thank Dr. V. Kavečanský (IEP SAS Košice, Slovakia) for gathering the powder diffraction pattern.

Notes and references

[#] The effect of the crystal field in the case of f-elements can be modelled in terms of the Stevens operators as follows

$$\hat{V}^{cf}(\hat{r}) = \sum_{k=0,2,4}^{2l} \sum_{q=0}^{+k} B_k^q \cdot \hat{O}_k^q(\hat{J}_z, \hat{J}_\pm)$$

where $\hat{O}_k^q$ are equivalent operators constructed only of the angular momentum operators; B_k^q are the potential constants; k – tensor rank, $q \geq 0$ – its component. This form is too complex to be applied to the magnetic data fitting. The simplest form containing only a single parameter is represented by eqn (1) and this has been used in data fitting. The results give a rough estimate of the dominating potential constant $B_2^0 = \Delta / 3$.

1 (a) R. Sessoli, D. Gatteschi, A. Caneschi and M. A. Novak, *Nature*, 1993, **365**, 141; (b) R. Sessoli, L. Hui, A. R. Schake, S. Wang, J. B. Vincent, K. Folting, D. Gatteschi and G. Christou, *J. Am. Chem. Soc*., 1993, **115**, 1804

2 (a) P. Zhang, Y.-N. Guo and J. Tang, *Coord. Chem. Rev*., 2013, **257**, 1728; (b) R. Sessoli and A. K. Powell, *Coord. Chem. Rev*., 2009, **253**, 2328; (c) H. L. C. Feltham and S. Brooker, *Coord. Chem. Rev*., 2014, **276**, 1; (d) N. Ishikawa, M. Sugita, T. Ishikawa, S.-Y. Koshihara and Y. Kaizu, *J. Am. Chem. Soc*., 2003, **125**, 8694; (e) D.N. Woodruff, R.E.P. Winpenny and R.A. Layfield, *Chem. Rev*. 2013, **113**, 5110; (f) J. Luzon and R. Sessoli, *Dalton Trans*. 2012, **41**, 13556; (g) L. Spree and A.A. Popov, *Dalton Trans*., 2019, **48**, 2861

3 (a) M. Atzori and R. Sessoli, *J. Am. Chem. Soc*., 2019, **141**, 11339; (b) S. V. Eliseeva and J.-C. G. Bunzli, *New J. Chem*., 2011, **35**, 1165; (c) W. Wernsdorfer and R. Sessoli, *Science*, 1999, **284**, 133; (d) F. Troiani and M. Affronte, *Chem. Soc. Rev*., 2011, **40**, 3119; (e) L. Bogani and W. Wernsdorfer, *Nature Mater*. 2008, **7**, 179

4 (a) T. Han, M. J. Giansiracusa, Z.-H. Li, Y.-S. Ding, N. F. Chilton, R. E. P. Winpenny and Y.-Z. Zheng, *Chem. Eur. J*., 2020, **26**, 6773; (b) D. Gatteschi, R. Sessoli and J. Villain, Molecular Nanomagnets, Oxford University Press, 2006

5 J. D. Rinehart and J. R. Long, *Chem. Sci*., 2011, **2**, 2078; (b) L. Li, J. Gou, D.-F. Wu, Y.-J. Wang, Y.-Y. Duan, H.-H. Chen, H.-L. Gao and J.-Z. Cui, *New J. Chem*., 2020, **44**, 3912

6 (a) Z.-H. Zhu, H.-L. Wang, X.-X. Fu, H.-H. Zou and F.-P. Liang, *Appl. Organomet. Chem*., 2020; e5808; (b) J. Lu, Y.-Q. Zhang, X.-L. Li, M. Guo, J. Wu, L. Zhao and J. Tang, *Inorg. Chem*. 2019, **58**, 5715; (c) Z. Jiang, L. Sun, M. Li, H. Wu, Z. Xia, H. Ke, Y. Zhang, G. Xie and S. Chen, *RSC Adv*., 2019, **9**, 39640; (d) K. N. Pantelis, P. S. Perlepe, S. Grammatikopoulos, C.

Lampropoulos, J. Tang and T. C. Stamatatos, *Molecules*, 2020, **25**, 2191; (e) O. Khalfaoui, A. Beghidja, J. Long, C. Beghidja, Y. Guari, J. Larionova, *Inorganics*, 2018, **6**, 35; (f) A. Vráblová, M. Tomás, L. R. Falvello, Ľ. Dlháň, J. Titiš, J. Černák and R. Boča, *Dalton Trans*., 2019, **48**, 13943; (g) R. Boča, M. Stolárová Pataky, L. R. Falvello, M. Tomás, J. Titiš and J. Černák, *Dalton Trans*., 2017, **46**, 5344

7 F.-S. Guo, B. M. Day, Y.-C. Chen, M.-L. Tong, A. Mansikkamäki and R. A. Layfield, *Science*, 2018, **362**, 1400

8 (a) C. A. P. Goodwin; F. Ortu; D. Reta; N. F. Chilton and D- P. Mills, *Nature*, 2017, **548**, 439; Y.-S. Ding, N. F. Chilton, R. E. P. Winpenny and Y.-Z. Zheng, *Angew. Chem. Int. Ed*., 2016, **55**, 16071

9 (a) S. Zhang, N. Shen, S. Liu, R. Ma, Y.-Q. Zhang, D.-W. Hu, X.-Y. Liu, J.-W. Zhang and D.-S. Yang, *CrystEngComm*, 2020, **22**, 1712; (b) F. Habiba and M. Murugesu, *Chem. Soc. Rev*., 2013, **42**, 3278; (c) Y.-N. Guo, G.-F. Xu, W. Wernsdorfer, L. Ungur, Y. Guo, J. Tang, H.-J. Zhang, L. F. Chibotaru and A. K. Powell, *J. Am. Chem. Soc*., 2011, **133**, 11948

10 (a) Y.-L. Hou, L. Liu, Z.-T. Hou, C.-Y. Sheng, D.-T. Wang, J. Ji, Y. Shi and W.-M. Wang, *Inorg. Chem. Commun*., 2020, **112**, 107691; (b) L. Qin, Y. Z. Yu, P. Q. Liao, W. Xue, Z. Zheng, X. M. Chen and Y. Z. Zheng, *Adv. Mater*., 2016, **28**, 10772; (c) X. Y. Li, H. F. Su, Q. W. Li, R. Feng, H. Y. Bai, H. Y. Chen, J. Xu and X. H. Bu, *Angew. Chem. Int. Ed*., 2019, **58**, 10184; (d) X.-Y. Zheng, J. Xie, X.-J. Kong, L.-S. Long and L.-S. Zheng, *Coord. Chem. Rev*., 2019, **378**, 222; (e) S. Biswas, S. Das, J. Acharya, V. Kumar, J. van Leusen, P. Kögerler, J. M. Herrera, E. Colacio and V. Chandrasekhar, *Chem. Eur. J*., 2017, **23**, 5154; (f) K. Katoh, T. Morita; N. Yasuda; W. Wernsdorfer, Y. Kitagawa; B. K. Breedlove and M. Yamashita, *Chem. Eur. J*., 2019, **25**, 3098

11 (a) R. A. Layfield and M. Murugesu, Lanthanides and Actinides in Molecular Magnetism. Wiley-VCH, Weinheim, Germany, 2015; (b) V. Vieru; L. Ungur and L. F. Chibotaru, *J. Phys. Chem. Let*., 2013, **4**, 3565

12 (a) B. Fernández, I. Oyarzabal, E. Fischer-Fodor, S. Macavei, I. Sánchez, J. M. Seco, S. Gómez-Ruiz and A. Rodríguez-Diéguez, *CrystEngComm*, 2016, **18**, 8718; (b) L. Zhong, W.-B. Chen, X.-H. Li, Z.-J. OuYang, M. Yang, Y.-Q. Zhang, S. Gao and W. Dong, *Inorg. Chem*., 2020, **59**, 4414; (c) M. Hojorat, H. Al Sabea, L. Norel, K. Bernot, T. Roisnel, F. Gendron, B. Le Guennic, E. Trzop, E. Collet, J. R. Long and S. Rigaut, *J. Am. Chem. Soc*., 2020, **142**, 931; (d) L. Zhong, W.-B. Chen, Z.-J. OuYang, M. Yang, Y.-Q. Zhang, S. Gao, M. Schulze, W. Wernsdorfer and W. Dong, *Chem. Commun*., 2020, **56**, 2590; (e) W. Gao, H. Huang, A.-M. Zhou, H. Wei, J.-P. Liu and X.-M. Zhang, *CrystEngComm*, 2020, **22**, 267; (f) C. Bai, C.-T. Li, H.-M. Hu, B. Liu, J.-D. Li and G. Xue, *Dalton Trans*., 2019, **48**, 814

13 (a) J. Wang, M. Yang, J. Sun, H. Li, J. Liu, Q. Wang, L. Li, Y. Ma, B. Zhao and P. Cheng, *CrystEngComm*, 2019, **21**, 6219; (b) J. Jung, F. Le Natur, O. Cador, F. Pointillart, G. Calvez, C. Daiguebonne, O. Guillou, T. Guizouarn, B. Le Guennic and K. Bernot, *Chem. Commun*., 2014, **50**, 13346; (c) X.-C. Huang, M. Zhang, D. Wu, D. Shao, X.-H. Zhao, W. Huang and X.-Y. Wang, *Dalton Trans*., 2015, **44**, 20834

14 C. R. Groom, I. J. Bruno, M. P. Lightfoot and S. C. Ward, *Acta Cryst*., 2016, **B72**, 171

15 T. Behrsing, G. B. Deacon, P. C. Junk, B. W. Skelton, A. N. Sobolev and A. H. White, *Z. Anorg. Allg. Chem*., 2013, **639**, 41

16 M. Stolárová, J. Černák, M. Tomás, I. Ara, M. Orendáč and L.R. Falvello, *Polyhedron*, 2015, **88**, 149

17 E. Gao, N. Sun, Y. Zhan, X. Qiu, Y. Ding, S. Zhang and M. Zhu, *RSC Advances*, 2016, **6**, 85704

18 X. Li, X.-S. Wu, H.-L. Sun, L.-J. Xu and G.-F. Zi, *Inorg. Chim. Acta*, 2009, **362**, 2837

19 X. Li, Y.-Q. Li, X.-J. Zheng and H.-L. Sun, *Inorg. Chem. Commun*., 2008, **11**, 779

20 K. Nakamoto, Infrared and Raman Spectra of Inorganic and Coordination Compounds, Part B: Applications in Coordination, Organometallic, and Bioinorganic Chemistry, 6th Ed., Wiley, New York, 1997

21 (a) A. Le Bail, H. Duroy and J. L. Fourquet, *Mater. Res. Bull*. 1988, **23**, 447; (b) V. Petříček, M. Dušek and L. Palatinus, *Z. Kristallogr*., 2014, **229**, 345

22 R. D. Shannon, *Acta Crystallogr*., 1976, **A32**, 751

23 J. Černák, K. Harčárová, M. Uličný, R. Tarasenko, M. Orendáč and L. R. Falvello, *J. Mol. Struct*., 2017, **1137**, 179

24 M. Llunell, D. Casanova, J. Cirera, P. Alemany, S. Alvarez, *SHAPE* - Program for the Stereochemical Analysis of Molecular Fragments by Means of Continuous Shape Measures and Associated Tools, Version 2.1, University of Barcelona, Spain, March 2013

25 P. Kalita, J. Goura, J. M. H. Martínez, E. Colacio and V. Chandrasekhar, *Eur. J. Inorg. Chem*., 2019, 212

26 Z.-Y. Li, B. Zhai, S.-Z. Li, G.-X. Cao, F.-Q. Zhang, X.-F. Zhang, F.-L. Zhang and C. Zhang, *Cryst. Growth Des*., 2016,**16**, 4574

27 M. Guo, Y. Xu, J. Wu, L. Zhao and J. Tang, Dalton Trans., 2017,46, 8252-8258

28 H. Ke, G.-F. Xu, Y.-N. Guo, P. Gamez, C. M. Beavers, S. J. Teatd and J. Tang, *Chem. Commun*., 2011, **13**, 6237

29 S. Roy, N. Hari and S. Sasankasekhar, *Eur. J. Inorg. Chem*., 2019, **29**, 3411

30 C. Rajnák, J. Titiš, J. Moncoľ, R. Mičová and R. Boča, *Inorg. Chem.*, 2019, **58**, 991-994

31 R. Boča, C. Rajnák, J. Titiš and D. Valigura, *Inorg. Chem.*, 2017, **56**, 1478-1482

32 R. Boča, C. Rajnák, J. Moncoľ, J. Titiš and D. Valigura, *Inorg. Chem.*, 2018, **57**, 14314−14321

33 J. Titiš, C. Rajnák, D. Valigura and R. Boča, *Dalton Trans.*, 2018, **47**, 7879-7882

34 C. Rajnák, J. Titiš, J. Moncoľ, F. Renz and R. Boča, *Eur. J. Inorg. Chem.*, 2017, 1520–1525

35 P.L. Scott and C. D. Jeffries, *Phys. Rev.*, 1962, **127**, 32-51

36 X. Qiu, X. Wang, S. Hou, H. Ma and Y. Tan, *J. Coord. Chem*., 2018, **71**, 1442

37 CrysAlisPro 1.171.38.46: Single-Crystal X-Ray Diffraction Data Collection and Processing Software, Rigaku OD, 2015

38 A. Altomare, G. Cascarano, C. Giacovazzo, A. Guagliardi, M. C. Burla, G. Polidori and M. Camalli, *J. Appl. Cryst*., 1994, **27**, 435

39 (a) G. M. Sheldrick, *Acta Cryst*., 2015, **C71**, 3; (b) G. M. Sheldrick, *Acta Cryst*., 2015, **A71**, 3

40 M. Nardelli, *J. Appl. Cryst*., 1995, **28**, 659

41 K. Brandenburg and H. Putz, 2008. Crystal Impact Diamond, Crystal and Molecular Structure Visualization, GbR, Postfach 1251, D-53002 Bonn, Germany

42 (a) F. Neese, The ORCA program system, *Wiley Interdiscip. Rev. Comput. Mol. Sci.,* 2012, **2**, 73; (b) F. Neese, ORCA – An Ab Initio, Density Functional and Semi-empirical Program Package, Version 4.1.2

43 M. Reiher and A. Wolf, *J. Chem. Phys.*, 2004, **121**, 2037

44 (a) D. Aravena, F. Neese and D. A. Pantazis, *J. Chem. Theory Comput*., 2016, **12**, 1148; (b) G. L. Stoychev, A. A. Auer and F. Neese, *J. Chem. Theory Comput*., 2017, **13**, 554

45 M. Atanasov, D. Aravena, E. Suturina, E. Bill, D. Maganas and F. Neese, *Coord. Chem. Rev.*, 2015, **289**, 177

View Article Online
DOI: 10.1039/D0NJ02276D

TOC

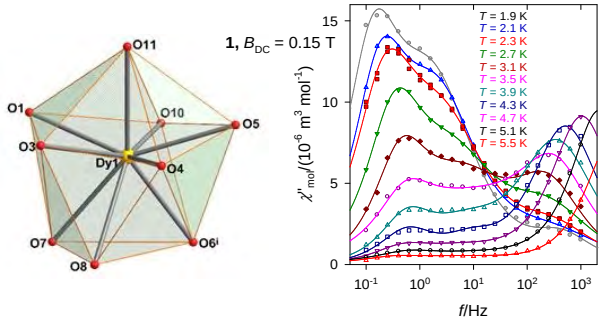

Three relaxation channels in field-induced SMM $[Dy(PDOA)(NO_3)(H_2O)_2]_n{\cdot}nH_2O$ with DyO_9 chromophore